

Supplementary Information

Single layers of WS₂ nanoplates embedded in
nitrogen-doped carbon nanofibers as anode materials
for lithium-ion batteries

*Sunmoon Yu, Ji-Won Jung, and Il-Doo Kim**

Department of Materials Science and Engineering, Korea Advanced Institute of Science and
Technology (KAIST), 291 Daehak-ro, Yuseong-gu, Daejeon 305-701, Republic of Korea

*E-mail: idkim@kaist.ac.kr

EXPERIMENTAL SECTION

Synthesis of materials: Ammonium tetrathiotungstate [ATTT, $(\text{NH}_4)_2\text{WS}_4$], polyacrylonitrile (PAN, $M_w = 150,000 \text{ g mol}^{-1}$) and N, N-dimethylformamide (DMF, 99.8%) were purchased from Sigma-Aldrich Co., Ltd. To prepare a precursor solution for single-spinneret electrospinning, ATTT (0.75 g) and PAN (0.5 g) were dissolved in DMF (5 ml). After vigorous stirring at 70 °C for 3 h, the electrospinning process was carried out. A distance of 15 cm between the needle of the spinneret (25 gauge) to the collector, a voltage of 15 kV, and a feeding rate of $5 \mu\text{l min}^{-1}$ were maintained. A two-step heat treatment was conducted under a reducing atmosphere (H_2/N_2 , 5%/95%, v/v). The obtained as-spun WS_2 precursor@PAN nanofibers (NFs) were annealed in a tubular furnace at 400 °C for 2 h and subsequently annealed at 700 °C for 5 h at a heating rate of 5 °C min^{-1} . The annealed product was designated as WS_2 @NCNFs. For comparison, N-doped carbon nanofibers (NCNFs) were synthesized without adding ATTP precursor, and bulk WS_2 powder was synthesized using the as-purchased ATTT precursor through the same two-step heat treatment without the electrospinning process.

Material characterization: The morphologies of the WS_2 precursor@PAN NFs and the WS_2 @NCNFs were observed by field-emission scanning electron microscopy (FE-SEM, Nova230, FEI). The crystal structures of the WS_2 @NCNFs and the WS_2 powder were determined by powder X-ray diffraction (XRD, D/MAX-2500, Rigaku). The WS_2 @NCNFs were further characterized by a thermogravimetry analyzer (TGA, TG 209 F3, NETZSCH) at a heating rate of 5 °C min^{-1} in air. A transmission electron microscope (TEM, Titan cubed G2 60-300, FEI) equipped with an energy dispersive spectrometer (EDS) was used to gather information on the internal microstructure and the atomic distribution of the WS_2 @NCNFs. Raman spectroscopy was measured on a Raman spectrometer with a 514 nm laser (FT-Raman,

Bruker), and the X-ray photoelectron spectroscopy (XPS) spectra was collected on an XPS spectrometer (K-alpha, Thermo VG Scientific). An elemental analysis was conducted using an element analyzer (EA, Flash 2000, Thermo Scientific).

Electrochemical characterization: The electrochemical performances of the WS₂@NCNFs and the WS₂ powder were evaluated in coin-type cells (2032, Hohsen), which were assembled in an argon-filled glove box. The anodes were composed of an active material, super P carbon black, and poly(acrylic acid)/sodium carboxymethyl cellulose (50%/50%, wt/wt, Aldrich) at a weight ratio of 75:15:10. The slurry was coated onto a Cu current collector and dried in a vacuum at 135 °C for 2h. Typical mass loading of the active materials was approximately 1.5 mg cm⁻². The whole weight of the coated composite material was used to calculate specific capacities. Lithium metal foil was used as the counter electrode, and the separator placed between the two electrodes was Celgard 2325. 1.3 M LiPF₆ in a 1:1 mixture (by volume) of ethylene carbonate (EC) and diethylene carbonate (DEC) (Soulbrain Co., Ltd., Korea) was used as the electrolyte. Cyclic voltammetry (CV) curves were collected at 0.1 mV s⁻¹ in a range of 0.01 to 3.0 V. The cells were galvanostatically charged and discharged between 0.01 and 3.0 V (vs. Li/Li⁺) at different current densities. During the electrochemical impedance spectroscopy (EIS) measurements, the AC amplitude was 10 mV and the applied frequency range was from 100 kHz to 1 Hz.

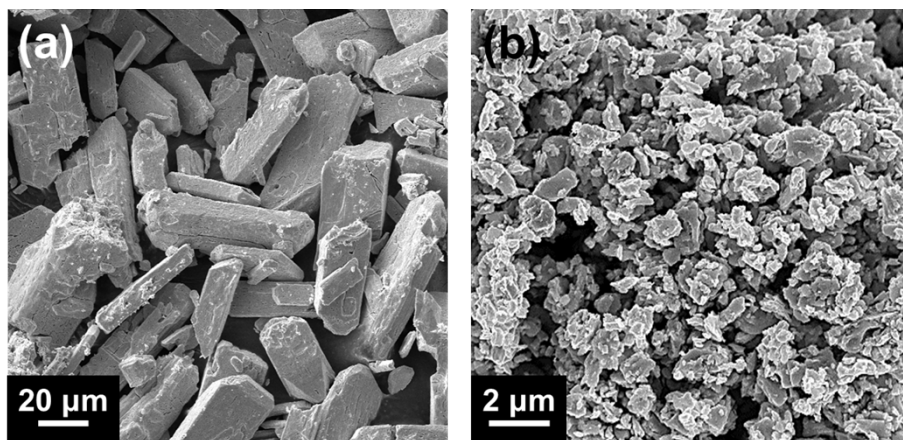


Fig. S1 Scanning electron microscopy (SEM) images of (a) WS₂ powder and (b) ground WS₂ powder.

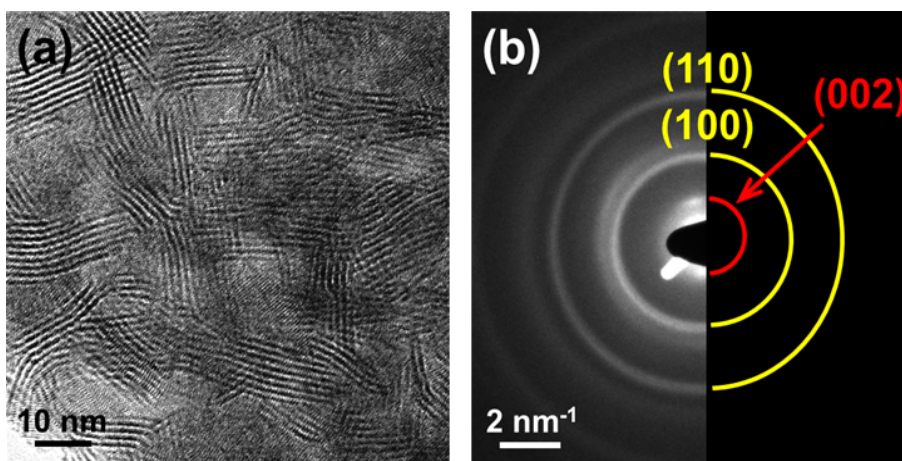


Fig. S2 (a) Transmission electron microscopy (TEM) image of WS₂ powder. (b) Selected area electron diffraction (SAED) pattern of the WS₂ powder.

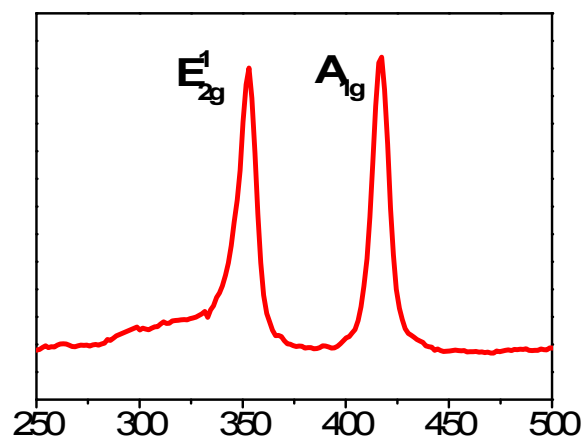


Fig. S3 Raman spectra of the WS₂ powder.

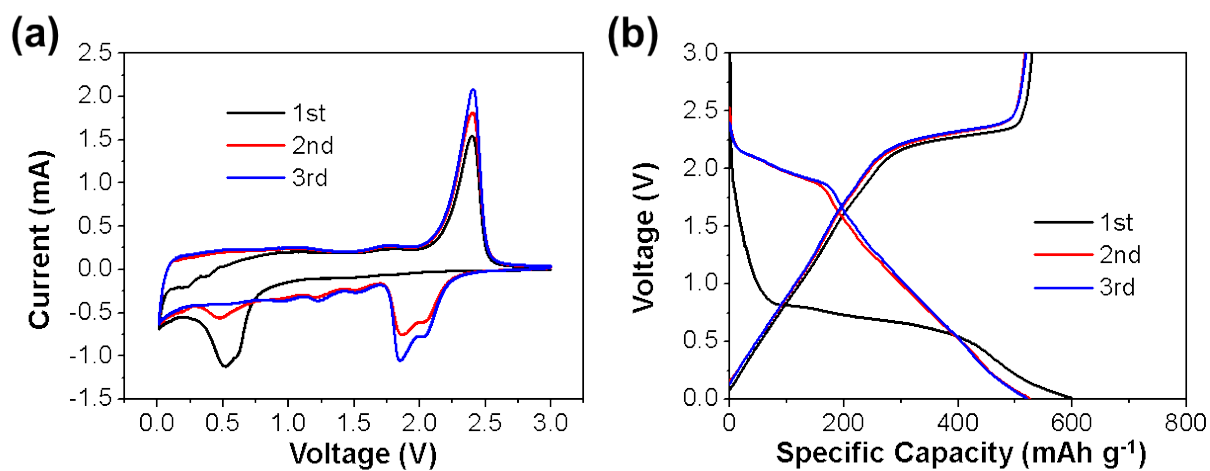


Fig. S4 (a) Cyclic voltammetry curves of the WS₂ powder over a voltage range of 0.01-3.0 V at a scanning rate of 0.1 mV s⁻¹. (b) Discharge/Charge voltage profile of the WS₂ powder at a current density of 0.1 A g⁻¹.

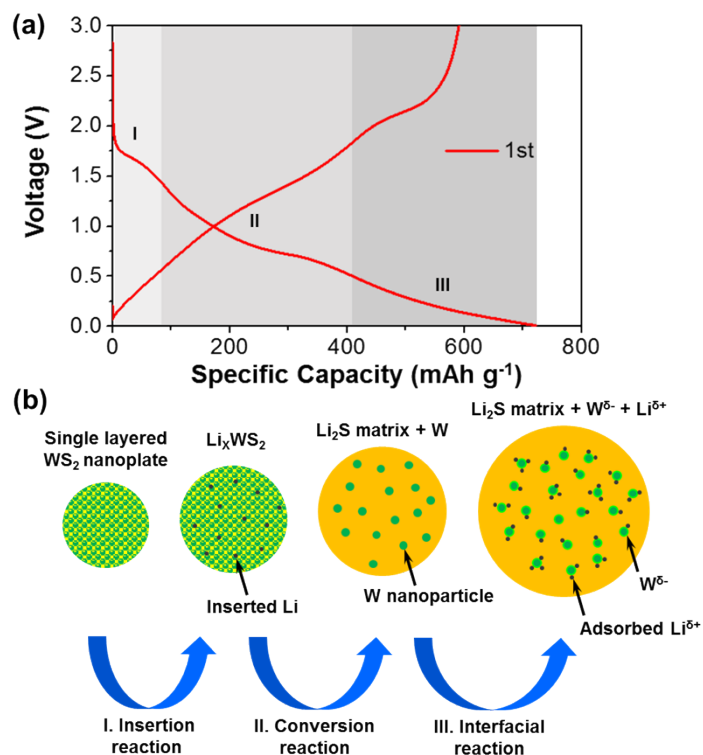


Fig. S5 (a) Discharge/charge profile for the first cycle of the WS₂@NCNFs at a current density of 0.1 A g⁻¹, divided into insertion, conversion, and interfacial reaction range. (b) Schematic diagram of a single layered WS₂ nanoplate which consecutively undergoes insertion, conversion, and interfacial reaction during lithiation.

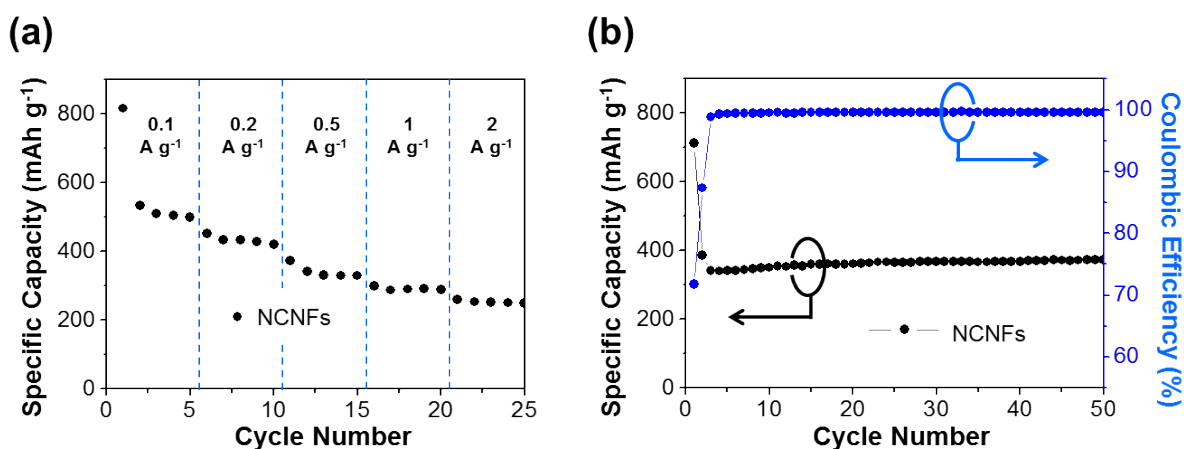


Fig. S6 (a) Rate capabilities of N-doped carbon nanofibers (NCNFs) at current densities of 0.1, 0.2, 0.5, 1, and 2 A g⁻¹. (b) Galvanostatic cycling performance and Coulombic efficiency of the NCNFs at a current density of 0.5 A g⁻¹.

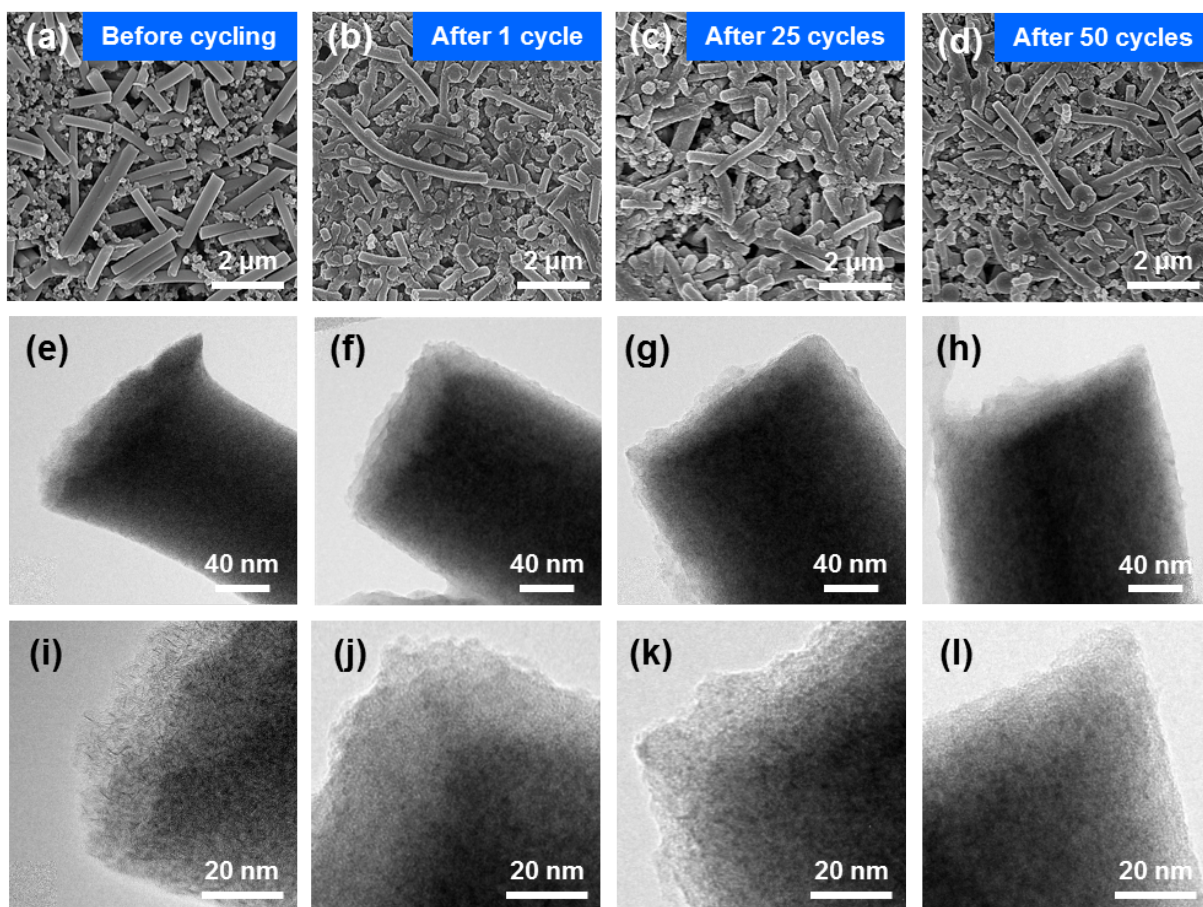


Fig. S7 SEM images, TEM images, and high-resolution TEM images of the $\text{WS}_2@\text{NCFNs}$ (a, e, and i) before cycling, (b, f, and j) after 1 cycle, (c, g, and k) after 25 cycles, and (d, h, and l) after 50 cycles, respectively.

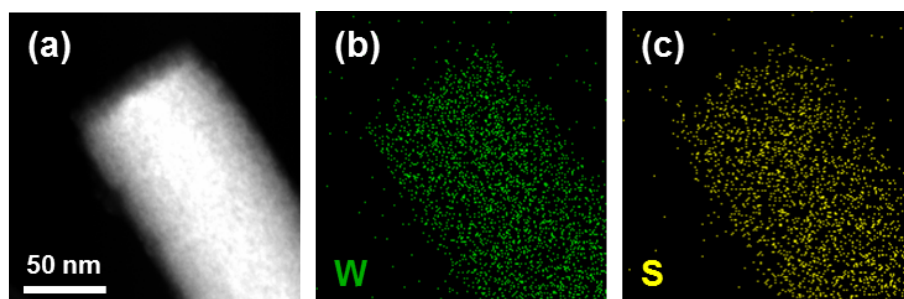


Fig. S8 (a) STEM image and (b and c) STEM-EDS mapping images of the $\text{WS}_2@\text{NCFNs}$ after 50 cycles: W (green) and S (yellow)

Table S1 Specific capacity of lithium storage for the WS₂@NCNFs, for the NCNFs, and for the single layered WS₂ nanoplates.

Current density (A g ⁻¹)	Measured capacity of WS ₂ @NCNFs (mAh g ⁻¹)	Measured capacity of NCNFs (mAh g ⁻¹)	Contribution of NCNFs (23 wt%) to the composite capacity (mAh g ⁻¹)	Contribution of WS ₂ (77 wt%) to the composite capacity (mAh g ⁻¹)	Calculated capacity of WS ₂ (mAh g ⁻¹)
0.1	596.2	491.4	113.0	483.2	627.5
0.2	580.0	428.9	98.6	481.4	625.1
0.5	541.0	329.5	75.8	465.2	604.2
1.0	496.0	289.9	66.7	429.3	557.6
2.0	367.1	250.2	57.5	309.6	402.0